JVI
Journals.ASM.org

Xpr1 Is an Atypical G-Protein-Coupled Receptor That Mediates Xenotropic and Polytropic Murine Retrovirus Neurotoxicity

Andrew E. Vaughan,[a] Ramon Mendoza,[a] Ramona Aranda,[a]* Jean-Luc Battini,[b] and A. Dusty Miller[a]

Human Biology Division, Fred Hutchinson Cancer Research Center, Seattle, Washington, USA,[a] and Institut de Génétique Moléculaire de Montpellier, CNRS-UMR 5535, Montpellier, France[b]

Xenotropic murine leukemia virus-related virus (XMRV) was first identified in human prostate cancer tissue and was later found in a high percentage of humans with chronic fatigue syndrome (CFS). While exploring potential disease mechanisms, we found that XMRV infection induced apoptosis in SY5Y human neuroblastoma cells, suggesting a mechanism for the neuromuscular pathology seen in CFS. Several lines of evidence show that the cell entry receptor for XMRV, Xpr1, mediates this effect, and chemical cross-linking studies show that Xpr1 is associated with the Gβ subunit of the G-protein heterotrimer. The activation of adenylate cyclase rescued the cells from XMRV toxicity, indicating that toxicity resulted from reduced G-protein-mediated cyclic AMP (cAMP) signaling. Some proteins with similarity to Xpr1 are involved in phosphate uptake into cells, but we found no role of Xpr1 in phosphate uptake or its regulation. Our results indicate that Xpr1 is a novel, atypical G-protein-coupled receptor (GPCR) and that xenotropic or polytropic retrovirus binding can disrupt the cAMP-mediated signaling function of Xpr1, leading to the apoptosis of infected cells. We show that this pathway is also responsible for the classic toxicity of the polytropic mink cell focus-forming (MCF) retrovirus in mink cells. Although it now seems clear that the detection of XMRV in humans was the result of sample contamination with a recombinant mouse virus, our findings may have relevance to neurologic disease induced by MCF retroviruses in mice.

XMRV (xenotropic murine leukemia virus-related virus) was initially discovered in human prostate cancer samples (36) and, more recently, in the blood of a high percentage of patients diagnosed with chronic fatigue syndrome (CFS) (20). Follow-up studies found an even higher percentage of CFS patients harboring murine leukemia virus (MLV) sequences in their peripheral blood cells (19), but these viral sequences were closely related to known endogenous MLVs and not to the XMRV isolates, adding confusion to the issue. Since these reports, many groups have been unable to confirm the presence of XMRV in humans with prostate cancer or CFS (1, 14). Moreover, while the specific sequence of XMRV initially appeared relatively unique to humans, a nearly identical virus was found in a common prostate cancer cell line, 22Rv1 (13), and new evidence indicates that this virus arose from recombination between two endogenous mouse viruses during the xenotransplantation of the cells in nude mice (27). The widespread use of 22Rv1 cells and plasmid clones of XMRV suggests that the detection of XMRV is due to experimental contamination with such materials.

Because it initially appeared that XMRV was indeed a new human retrovirus, we began studies to understand potential disease mechanisms. We first tested XMRV for a possible transforming activity that might explain a role for XMRV in prostate cancer but found no evidence that XMRV was acutely oncogenic (22). We next explored the possibility that XMRV was neurotoxic and that this might explain a role for XMRV in the neuromuscular disease aspects of CFS. Indeed, several MLVs are known to have neurologic and cytotoxic effects in animals and in cultured cells (32). Some MLVs cause paralytic motor neuron disease in mice, and the envelope (Env) proteins of these viruses are often mechanistically involved. For example, CasBr-E MLV induces spongiform neurodegeneration that is thought to involve an interaction between the viral Env protein and its cognate receptor mCAT-1 (17). Similarly, the Fr98 polytropic Friend MLV induces astrogliosis in mice, and this neurovirulence is critically dependent on specific amino acid residues in the Env protein (30, 31). We sought to determine if XMRV had a similar cytotoxic potential *in vitro* and to examine potential mechanisms thereof.

The entry of xenotropic and polytropic retroviruses is mediated by the xenotropic and polytropic cell surface receptor Xpr1 (2, 35, 39), which has no documented function in higher eukaryotes. While of unknown function, orthologs of Xpr1 are present in many organisms and include the *Saccharomyces cerevisiae* protein Syg1. In yeast, Syg1 is thought to be a transmembrane signaling component that can respond to, or transduce signals through, the Gβ subunit of the G-protein trimer (34). This is evidenced by the ability of a Syg1 truncation mutant, and, to a lesser degree, the overexpression of wild-type Syg1, to suppress the lethality of a Gα deficiency.

G-protein signaling is important for a number of cellular processes, including neurotransmission, metabolism, growth, and apoptosis (8). Based on its homology to Syg1, we hypothesized that Xpr1 might play a similar role in G-protein signaling in mammalian cells and that xenotropic and polytropic MLV Env binding to Xpr1 might disrupt its normal function. Here we show that Xpr1 does participate in G-protein signaling and that XMRV or polytropic retrovirus binding to Xpr1 in a human neuronal cell line, and polytropic retrovirus binding to Xpr1 in mink cells, induces apoptosis by the downregulation of cyclic AMP (cAMP)-mediated G-protein signaling.

Received 19 August 2011 **Accepted** 8 November 2011
Published ahead of print 16 November 2011
Address correspondence to A. Dusty Miller, dmiller@fhcrc.org.
* Present address: Undergraduate Program, New Mexico State University, Las Cruces, New Mexico, USA.

doi:10.1128/JVI.06073-11

MATERIALS AND METHODS

Cell culture. Cells were grown in Dulbecco's modified Eagle medium (DMEM) with 10% fetal bovine serum (FBS), with the following exceptions. SY5Y cells (SH-SY5Y; ATCC CRL-2266) (3) were grown in a 1:1 mixture of DMEM and Ham's F12 medium plus 15% FBS. Chinese hamster ovary (CHO-K1) cells (11), which require proline for growth, were grown in DMEM with 10% FBS and 1× nonessential amino acids (Gibco). For studies of phosphate uptake and its regulation, CHO cells and 208F rat fibroblasts (31a) were grown in DMEM without phosphate, 10% dialyzed FBS (to remove phosphate), and nonessential amino acids for the CHO cells.

Viruses. XMRV was obtained from 22Rv1 cells (ATCC CRL-2505), which constitutively produce XMRV (13). New Zealand black mouse (NZB) xenotropic retrovirus was made by the transfection of *Mus dunni* tail fibroblast (MDTF) cells (15a) with the NZB-9-1 plasmid (26). Because this plasmid contains a permuted copy of the NZB virus that was cloned by using the EcoRI site in the *env* gene, the plasmid was cut with EcoRI and religated to generate intact copies of the virus prior to transfection. After transfection, the cells were grown for 2 weeks to allow virus spread throughout the culture. MCF 98D virus was produced from MDTF cells infected with a biological clone of the virus (98D13) (a gift from Bruce Chesebro) (5). The LAPSN retroviral vector consists of the human placental alkaline phosphatase cDNA cloned into the LXSN expression vector (24). All retroviruses were produced by feeding confluent layers of virus-producing cells, harvesting the culture medium 12 to 24 h later, and filtering the medium through 0.45-μm-pore-size low-protein-binding filters to remove cells and debris. Viruses were stored at −70°C.

Construction of hybrid amphotropic/MCF viruses. Plasmids containing an amphotropic MLV provirus in which the *env* region was replaced with that of the MCF 98D virus were made by replacing the SphI-to-ClaI region in the amphotropic virus in plasmid pAMS (23) (GenBank accession number AF010170) with the SphI-to-ClaI regions of several MCF 98D virus clones (GenBank accession number AF133256) (kindly provided by Bruce Chesebro). This region contains 640 bp of the *pol* gene that is upstream of the *env* coding region and all but 100 bp of the end of the *env* coding region. In the hybrid virus, the end of the MCF virus *env* coding region downstream of the ClaI site was replaced with the nearly identical region of the amphotropic *env* gene. Virus was made from these plasmids by the transfection of MDTF cells, followed by the passage of the cells for >2 weeks to allow the virus to spread.

Analysis of apoptotic cells. SY5Y cells were seeded into 12-well plates at 5×10^4 cells per well, and the medium was replaced 1 day later. Two days after cell seeding, 100 μl of virus (~10^6 infectious units) was added to each well with 4 μg/ml Polybrene to increase the infection efficiency. The medium was replaced 1 day after infection. Three days after infection, nonadherent cells were harvested and combined with adherent cells harvested by using trypsin, and the cells were analyzed for annexin V binding by flow cytometry according to the manufacturer's protocol (Invitrogen). In experiments utilizing forskolin, cells were pretreated for 24 h and maintained in 50 μM forskolin.

Generation of retroviral vectors for expression of Xpr1 and Xpr1 truncation mutants. Xpr1 cDNAs from human (hXpr1), *Mus musculus* (mXpr1), and *Mus dunni* (mdXpr1) (GenBank accession numbers AF099082, AF198104, and AF198105, respectively) were cloned into the LXSN retroviral expression vector (24). C-terminal truncation mutants of human Xpr1, resulting in 200-, 229-, and 248-amino-acid (aa) proteins, were made by site-directed mutagenesis and were cloned into the LXSN vector. The structures of the inserts were verified by DNA sequencing. Virus was made from the vector plasmids by the transient transfection of 293 cells or by the generation of stable retrovirus packaging cell lines producing the vectors.

Cre-SEAP reporter assay. HEK 293 cells carrying the cAMP-responsive pCre-SEAP reporter plasmid (a generous gift from Linda Buck) (18) were generated by the cotransfection of pCre-SEAP with a plasmid carrying the *neo* gene, followed by the selection of the cells in G418 medium. Clonal cell lines were isolated, and one that showed the highest increase in the level of secreted alkaline phosphatase (SEAP) production (12-fold) in response to overnight treatment with 15 μM forskolin, which increases cAMP levels by the direct stimulation of adenylate cyclase, was chosen for subsequent experiments.

For the SEAP assay, HEK 293/Cre-SEAP cells were seeded at 250,000 cells per well in 24-well plates. On the following day, 0.5 ml of Xpr1-expressing or control retroviral vectors was added to each well with 4 μg/ml Polybrene, and the cells were incubated overnight. On the following day, each plate was covered with plastic wrap and incubated at 68°C for 2 h. Next, 0.5 ml of 2 M diethanolamine (pH 10) containing 1.2 mM 4-methylumbelliferyl phosphate was added to each well, and the cells were suspended by vigorous pipetting. Fluorescence was measured every 30 min with a Fluoroskan Ascent instrument with excitation at 360 nm and emission at 440 nm. Endpoint readings for each experiment were taken 3 h after the addition of the substrate.

Coimmunoprecipitation. NZB and amphotropic MLV Env SU-human IgG Fc hybrid proteins were produced as previously described (2, 15). The IgG Fc-tagged SU proteins were concentrated to a final concentration of 10 μg/ml by using Hi-Trap protein G columns according to the manufacturer's protocol (GE Healthcare).

Nearly confluent SY5Y cells were harvested by using phosphate-buffered saline (PBS) without calcium or magnesium and containing 1 mM EDTA. Cells were washed and resuspended in DMEM without serum, and 10^6 cells per assay were incubated with 2 μg of the Env SU hybrid protein in a 0.5-ml volume for 1 h at 4°C. Cells were washed once with DMEM and once with PBS, resuspended in 1 ml PBS containing 2 mM dithiobis(succinimidyl propionate), and incubated for 30 min at 25°C to cross-link proteins. Next, 20 μl of 1 M Tris (pH 7) was added to each sample to stop the cross-linking reaction, and samples were centrifuged at 800 × *g* for 10 min. Samples were then resuspended in 0.5 ml lysis buffer (20 mM HEPES, 100 mM NaCl, 1 mM EDTA, 1% sodium dodecyl sulfate [SDS], and protease inhibitors) and incubated for 1 h at 4°C.

Meanwhile, protein G-Sepharose beads (GE Healthcare) were washed twice in lysis buffer and then blocked at 4°C with lysis buffer containing 1% bovine serum albumin and 1% SDS for 1.5 h. The beads were then washed twice in lysis buffer and were resuspended a final time in lysis buffer without SDS. Cross-linked protein samples were centrifuged at 15,000 × *g* for 20 min to pellet insoluble material, and 50-μl aliquots of each sample were saved for the input controls. Fifty microliters of protein G-Sepharose beads was added to the remainder of each sample and incubated overnight at 4°C with continuous rotation. On the following day, the unbound lysate was discarded, and the beads were washed six times with lysis buffer plus 0.1% Tween 20, 0.1% Triton X, and 0.5% SDS. Samples were finally resuspended in 50 μl lysis buffer containing 1% SDS. Loading buffer containing β-mercaptoethanol was added to each sample and incubated at 37°C for 30 min, followed by incubation at 95°C for 15 min. Samples were loaded onto a 15% SDS-PAGE gel. After transfer, gels were probed with a pan-Gβ antibody (sc-378; Santa Cruz Biotechnology), followed by an anti-rabbit horseradish peroxidase (HRP) secondary antibody (P0448; Dako), and developed by using ECL Plus reagents (Amersham).

Phosphate uptake assays. CHO cells and 208F rat fibroblasts were transduced with Xpr1-expressing retroviral vectors and were selected in G418 medium. Cells were seeded at 2×10^5 to 4×10^5 cells per 3.5-cm-diameter dish in medium with various concentrations of [^{32}P]phosphate. Phosphate uptake was measured 1 day later, as previously described (12).

Statistical analysis. Statistical significance was determined by one-way analysis of variance (ANOVA) and by using the Tukey method to compare pairs of means. Calculations were made using GraphPad InStat 3 software.

RESULTS

XMRV induces apoptosis in SY5Y neuroblastoma cells. To assay for neurotoxicity that might be caused by XMRV, we infected

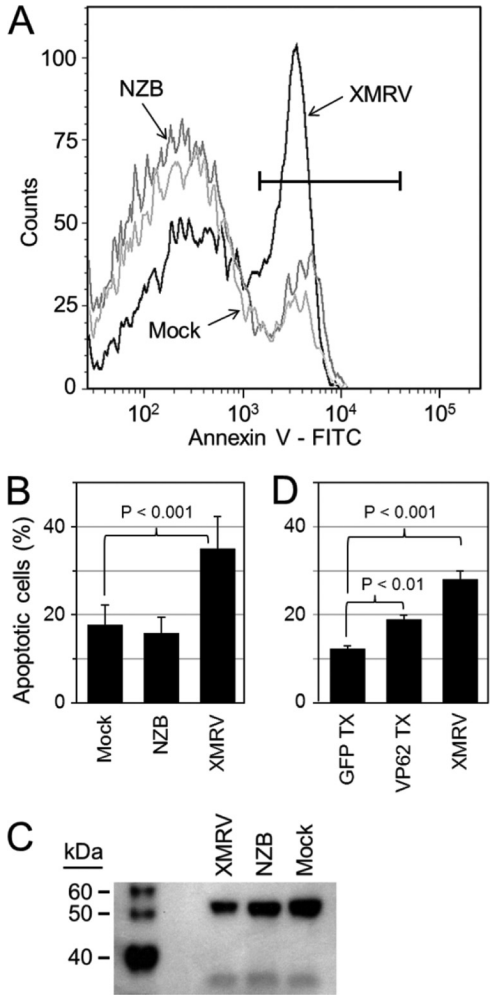

FIG 1 XMRV induces apoptosis in SY5Y cells. (A) Representative fluorescence-activated cell sorter (FACS) histogram showing annexin V staining of SY5Y cells 3 days after infection with the indicated retroviruses. The black bar represents the gate used to determine the percentage of apoptotic cells. FITC, fluorescein isothiocyanate. (B) Quantitation of apoptosis measured by FACS analysis 3 days after infection. Results are means ± standard deviations (SD) from 7 experiments. (C) XIAP expression 3 days after retrovirus infection of SY5Y cells was determined by Western blotting using equal amounts of total cell protein (Bradford assay [4a]) and XIAP antibody (catalog number 610762; BD Biosciences). (D) Quantitation of apoptosis by FACS analysis 3 days after exposure of SY5Y cells to medium made by the transfection of the VP62 XMRV plasmid (VP62 TX) or a control plasmid expressing GFP (GFP-TX) or to medium containing XMRV from 22Rv1 cells. Results are means ± SD from 2 experiments.

various neural cell lines with conditioned medium harvested from the 22Rv1 cell line, which produces high-titer XMRV (13). Daoy medulloblastoma (10), U-251 glioma (4), and HEK 293 neuronal-lineage (33) cells appeared to be unaffected by XMRV infection, while SY5Y neuroblastoma cells (3) displayed significant cell death starting 2 days after XMRV infection. By 3 days after infection, measurements of apoptosis by annexin V staining revealed that many more XMRV-infected cells had become apoptotic than mock-infected cells or cells infected with a related xenotropic retrovirus endogenous to NZB mice, NZB-9-1 (26) (Fig. 1A and B). X-linked inhibitor of apoptosis protein (XIAP) binds and inhibits several caspases in healthy cells, and lower levels of XIAP are characteristic of cells undergoing apoptosis. Consistent with the annexin V staining results, XMRV infection resulted in a lower level of the XIAP protein in SY5Y cells (Fig. 1C). The XIAP level of cells infected with the NZB virus was between that of mock-infected cells and that of XMRV-infected cells, suggesting that the NZB virus might also be somewhat toxic to SY5Y cells.

To address the possibility that 22Rv1 cells produced something in addition to XMRV that was responsible for the SY5Y cell toxicity that we observed, we produced XMRV from the VP62 XMRV clone (7) and tested this virus for toxic effects on SY5Y cells. To obtain virus with a high-enough titer for this experiment, we transfected HEK 293 cells with the VP62 clone or a plasmid expressing green fluorescent protein (GFP) as a control, exposed HT-1080 cells to medium from the transfected 293 cells, passaged the HT-1080 cells for several weeks, and exposed SY5Y cells to medium from the HT-1080 cells. The exposure of SY5Y cells to medium made by the transfection of the VP62 plasmid (VP62 TX) resulted in significantly more apoptosis than that produced by medium made by the transfection of the control GFP plasmid (GFP TX) (Fig. 1D), showing that XMRV can indeed induce SY5Y cell apoptosis. The titer of the VP62 virus measured by an S^+L^- assay (7×10^5) was lower than that of XMRV produced by 22Rv1 cells (3×10^6), which correlates with the lower toxicity of the VP62 virus than that of the XMRV produced by 22Rv1 cells. Because of its higher titer, we used XMRV from the 22Rv1 cells for the experiments described below.

Expression of mouse Xpr1 protects SY5Y cells from XMRV-induced apoptosis. The Env proteins of several retroviruses are known to affect normal receptor function. For example, the Env protein of the 4070A amphotropic MLV can inhibit phosphate uptake mediated by its receptor, Pit-2 (also called Ram-1 or SLC20A2) (12). To address the hypothesis that XMRV might cause cell death by affecting the function of its receptor, SY5Y cells were transduced with a retroviral vector expressing Xpr1 cloned from laboratory mice (mXpr1). While closely related to human Xpr1 (hXpr1), mXpr1 is unable to mediate the entry of xenotropic retroviruses and presumably is unable to bind the xenotropic MLV Env protein. We found that SY5Y cells expressing mXpr1 exhibited much less apoptosis following XMRV infection than did SY5Y cells transduced with the empty vector or a vector expressing hXpr1 (Fig. 2). The mXpr1-transduced SY5Y cells remained as susceptible to infection by XMRV as wild-type cells (XMRV-pseudotyped LAPSN vector titers of 4.1×10^4 and 3.9×10^4, respectively; $n = 2$), indicating that the SY5Y/mXpr1 cells still expressed endogenous hXpr1 at levels similar to those of SY5Y cells. These results show that mXpr1 can protect SY5Y cells from XMRV-induced apoptosis, presumably by compensating for the loss of hXpr1 function that occurs following the binding of XMRV Env to hXpr1, and indicate that hXpr1 plays a key role in the induction of apoptosis in SY5Y cells.

Xpr1 participates in G-protein-mediated cAMP signaling. Based on the similarity of Xpr1 to Syg1, a yeast G-protein interactor involved in cAMP signaling, we measured cAMP levels after the overexpression of human and mouse Xpr1 homologs in HEK 293 cells. To measure cAMP levels, the cells were transfected with the cAMP-responsive reporter Cre-SEAP and were selected for stable reporter expression. These reporter cells were then transduced with retroviral vectors that express Xpr1 genes at high levels. The overexpression of both hXpr1 and mXpr1 resulted in

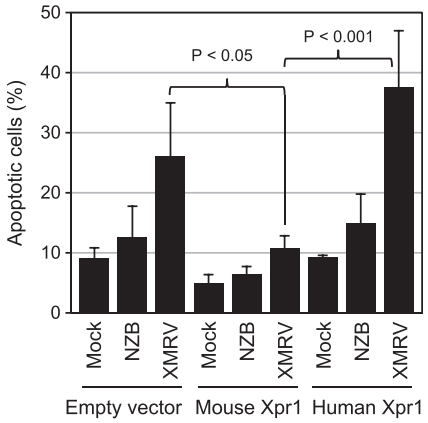

FIG 2 Expression of mXpr1 protects SY5Y cells from XMRV-induced apoptosis. SY5Y cells transduced with retroviral vectors encoding the indicated Xpr1 proteins or the empty vector were exposed to medium containing the indicated retroviruses or fresh medium only (mock), and the percentages of apoptotic cells were measured 3 days later. Results are means ± SD from two (empty vector and human Xpr1) or three (mouse Xpr1) experiments.

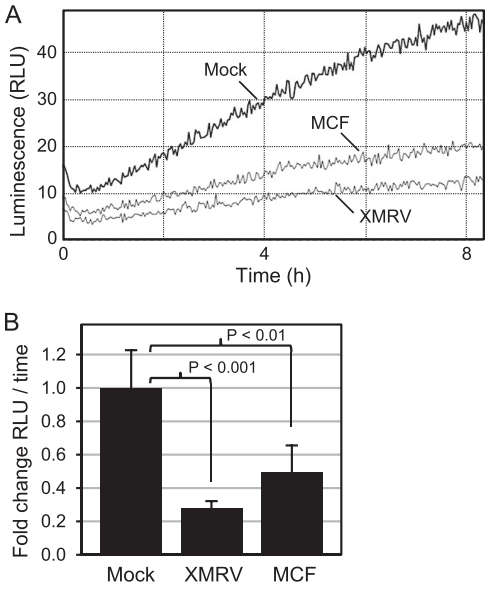

FIG 4 XMRV and MCF 98D virus infection of SY5Y cells decreases intracellular cAMP levels. (A) SY5Y cells containing the Glosensor cAMP 22F reporter construct were infected with virus and assayed for luciferase activity 3 days later. Luminescence as a function of time following the addition of luciferin to the cells is plotted. Each line represents the average of data from three wells in a 96-well plate. RLU, relative light units. (B) Fold changes in rates of luminescence gain relative to those of mock-infected cells are shown. Results are means ± SD from two experiments.

significantly higher levels of intracellular cAMP, as determined by SEAP expression from the reporter (Fig. 3A).

We reasoned that, like Syg1, Xpr1 might be inducing higher levels of cAMP by binding the Gβ subunit of the G-protein complex and liberating Gα to activate adenylate cyclase. We first attempted to use Xpr1 antibodies to coimmunoprecipitate proteins bound to Xpr1, but none of the commercially available Xpr1 antibodies bound Xpr1. Instead, we performed coimmunoprecipitation by using a hybrid protein consisting of the NZB Env extracellular domain (SU) linked to a human IgG constant fragment that is known to specifically bind Xpr1 (2). The NZB virus SU fusion protein bound in a complex to Gβ, whereas an equivalent fusion protein containing an amphotropic retrovirus Env SU, which binds the unrelated retrovirus receptor Pit-2 (15), did not show significant binding (Fig. 3B). These results show that Xpr1 associates with the Gβ component of the G-protein heterotrimer.

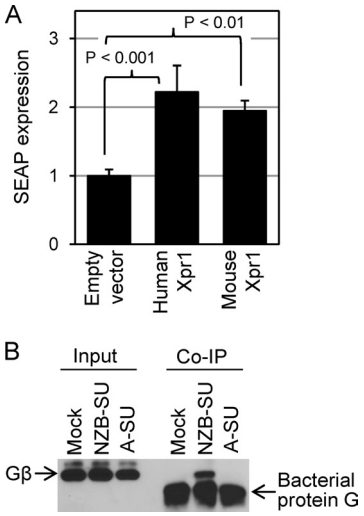

FIG 3 Overexpression of mXpr1 or hXpr1 increases cAMP levels, and hXpr1 is associated with the Gβ G-protein subunit. (A) cAMP levels in HEK 293 cells were measured by using the Cre-SEAP reporter 24 h after transduction with vectors encoding mXpr1 or hXpr1 or with the empty vector, as indicated. Results are means ± SD from three independent experiments. (B) SY5Y cells were incubated with IgG Fc-tagged NZB virus or amphotropic retrovirus Env SU proteins or with no protein (mock). Total proteins were cross-linked, coimmunoprecipitated using anti-IgG Fc antibody, and analyzed for the presence of the Gβ protein by Western blotting with a pan-Gβ antibody. Proteins present in the cell lysate made after protein cross-linking (input) and after coimmunoprecipitation (Co-IP) are shown. Lower bands in the coimmunoprecipitation lanes are due to dissociated bacterial protein G from the Sepharose beads. Input lanes indicate equivalent amounts of Gβ in the cell lysates prior to coimmunoprecipitation.

XMRV infection decreases intracellular cAMP levels. We hypothesized that XMRV toxicity in SY5Y cells is mediated by reduced cAMP levels resulting from XMRV Env binding to Xpr1 and the resultant inhibition of Xpr1 signaling. To test directly for reduced cAMP levels, we utilized the Glosensor cAMP 22F system to analyze cAMP levels in SY5Y cells. The Glosensor reporter consists of a luciferase enzyme that is activated directly in proportion to the intracellular cAMP level. The infection of Glosensor-expressing SY5Y cells with XMRV resulted in lower rates of luminescence increases, indicative of lower levels of luciferase (Fig. 4A and B) and, therefore, lower intracellular cAMP levels. Similarly, the polytropic MCF 98D retrovirus (5), which also binds Xpr1 but takes longer to induce apoptosis in SY5Y cells (9 days after infection, compared to 3 days for XMRV), also reduced cAMP levels although not to the same degree as XMRV.

Increased levels of cAMP protect cells from XMRV-induced apoptosis. To further test the hypothesis that XMRV induces apoptosis by downregulating cAMP levels in SY5Y cells, we treated cells with forskolin, a direct activator of adenylate cyclase, and then infected the cells with XMRV. In contrast to untreated cells, forskolin treatment significantly decreased the size of the apoptotic population of cells 3 days after infection (Fig. 5). This

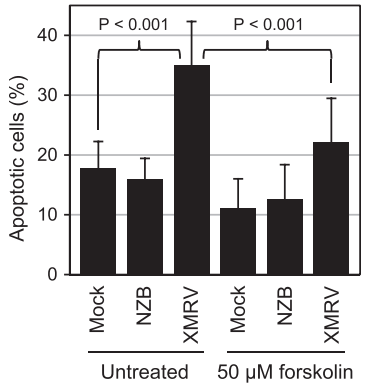

FIG 5 Forskolin protects SY5Y cells from XMRV toxicity. SY5Y cells were cultured with or without 50 μM forskolin for 24 h prior to infection and for 72 h after infection with the indicated viruses. Results are means ± SD from seven experiments. Note that the data for untreated (no forskolin) cells are also shown in Fig. 1B. The statistical analysis depicted here was performed by ANOVA using all data from untreated and treated cells, while that for Fig. 1B used only the data for untreated cells.

indicates that an increase of the cAMP level protects cells from XMRV-induced apoptosis. Forskolin treatment also appeared to decrease the basal level of apoptosis in mock-infected SY5Y cells (Fig. 5), although this trend was not statistically significant ($P >$ 0.05), suggesting that SY5Y cells constitutively maintain levels of cAMP that are insufficient to prevent apoptosis.

Expression of carboxy-terminally deleted Xpr1 mutants protects SY5Y cells against XMRV-induced apoptosis. C-terminally truncated forms of Syg1 in yeast are known to suppress the lethality of a Gα subunit deficiency by stimulating constitutive signaling through Gβ (34). In fact, two of the truncated proteins (400 and 417 aa) were found to be more active than full-length Syg1. To test whether Xpr1 might have similar properties, we made similar C-terminal truncation mutants of Xpr1 (200, 229, and 248 aa) by reference to the hydropathy plots of both proteins (Fig. 6A). Note that the lengths of Xpr1 and Syg1 are quite different (696 and 902 aa, respectively), with most of the difference being in the N-terminal presumed cytoplasmic domain. The Xpr1 mutants were cloned into a retroviral expression vector, and vesicular stomatitis virus G-protein (VSV-G)-pseudotyped vector preparations were made for each of the mutants, for full-length hXpr1, and for the empty vector. SY5Y cells were transduced with the vectors, grown in G418 medium to select for the expression of the *neo* gene present in all of these vectors, and tested for resistance to XMRV-induced apoptosis. In contrast to SY5Y cells transduced with the vector alone, those expressing the Xpr1 truncations showed significantly reduced apoptotic populations after XMRV infection (Fig. 6B). Basal levels of apoptosis appeared to be reduced in cells expressing the truncation mutants (Fig. 6B), although this difference was not statistically significant ($P >$ 0.05). This effect is similar to the effect observed following forskolin treatment (Fig. 5) and suggests that the Xpr1 truncation mutants can increase constitutive cAMP levels and thereby decrease apoptosis.

Polytropic and xenotropic viruses can kill Mv1Lu mink lung cells. MCF polytropic retroviruses are well known to be toxic to Mv1Lu mink lung epithelial cells in tissue culture (9, 40). Indeed, this toxicity is the basis for the mink cell focus assay used to quantitate MCF viruses (9). It was proposed previously that this death is due to virus superinfection and the subsequent buildup of the

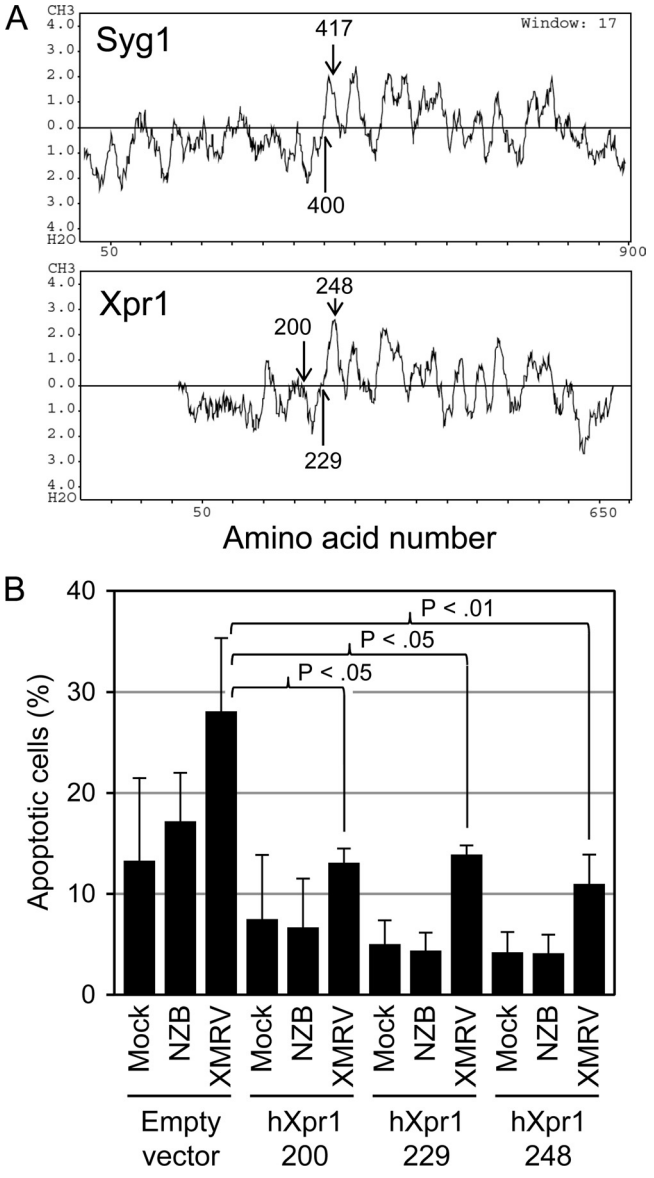

FIG 6 Truncation mutants of Xpr1 provide protection against XMRV-induced apoptosis. (A) Hydropathy plots of the yeast (*S. cerevisiae*) Syg1 and human Xpr1 proteins are shown. The Xpr1 plot was shifted to the right to align the first putative transmembrane domain of each protein. The locations of the last amino acids of the C-terminal truncation mutations are shown. The 400- and 417-aa Syg1 truncations were found to be fully active in yeast (34). (B) SY5Y cells transduced with retroviral vectors encoding the indicated hXpr1 truncation mutants, or the empty vector, were cultured and infected with the indicated retroviruses. Three days after infection, the percentages of apoptotic cells were measured by annexin V staining and flow cytometry. Results are means ± SD from three independent experiments.

Env protein, resulting in endoplasmic reticulum (ER) stress (41). However, given the similarities between this phenomenon and XMRV toxicity to SY5Y cells, we hypothesized that MCF virus might kill cells via a similar cAMP-mediated mechanism.

We first tested for xenotropic retrovirus toxicity to mink cells in comparison to the known MCF virus toxicity. Cells infected with the MCF 98D virus showed obvious toxicity within 3 to 5 days, with nearly complete cell death within the next week. XMRV

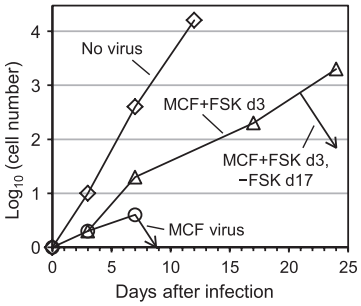

FIG 7 Forskolin protects mink cells from polytropic (MCF) virus-induced death. Twenty-percent-confluent Mv1Lu mink lung epithelial cells (ATCC CCL-64) were exposed to ~10^7 infectious units of MCF 98D virus or no virus in the presence of 4 μg/ml Polybrene. Cells were trypsinized and seeded at 1:10 and 1:40 dilutions every time they reached confluence. Cells were visually monitored daily for the presence of any cytopathic effects and cell death. Cells were treated with 25 μM forskolin (FSK) as indicated. Cell numbers were normalized to the starting cell number and were approximated based on the time that it took to reach confluence again after a 1:10 or 1:40 split. Results using two different preparations of MCF virus harvested from MDTF cells infected with the MCF 98D virus were the same.

showed limited toxicity that was not apparent until 18 days after infection. NZB virus infection showed intermediate toxicity, with cell death being apparent in 11 to 12 days. Note that we previously reported that XMRV infection was not toxic to mink cells (22), but the virus used for infection in that study was a mixture of XMRV and the LAPSN vector. The LAPSN vector replicates more efficiently than XMRV in coinfected cells (22), and this may explain why the virus mixture showed no toxic effects. In contrast, pure XMRV reproducibly induced toxicity in mink cells.

Forskolin treatment protects mink lung cells and SY5Y neuroblastoma cells from polytropic retrovirus-induced death. To determine whether cAMP levels play a role in polytropic retrovirus toxicity in mink cells, mink cells were infected with the MCF 98D virus, and when toxicity was apparent on day 3, the cells were trypsinized and replated with or without 25 μM forskolin, which directly stimulates cAMP production. The MCF virus-infected mink cells treated with forskolin resumed their growth, while those without forskolin continued to exhibit toxicity and were mostly dead by day 10 after infection (Fig. 7). The forskolin-treated MCF virus-infected cells continued to grow, although not as quickly as uninfected mink cells, until the experiment was terminated on day 24. On day 17, when these cells were trypsinized and reseeded, some cells were cultured in parallel without forskolin. The cells grown with and those grown without forskolin appeared to grow at similar rates until day 21, after which most of the cells grown without forskolin died (Fig. 7). These results show that forskolin, a direct activator of adenylate cyclase, can reverse MCF retrovirus-induced toxicity in mink cells.

We performed additional experiments to test for a role of cAMP in SY5Y killing by the MCF 98D polytropic retrovirus. Although it took longer for the MCF 98D virus to kill SY5Y cells than XMRV (9 and 2 days, respectively), killing by the MCF 98D virus was dramatic. At day 12, when most of the MCF virus-infected cells were dead, we trypsinized and replated the cells with or without 50 μM forskolin, after which the forskolin-treated cells recovered and grew well until the experiment was terminated 1 week later, while the untreated cells continued to die. Overall, these results indicate that decreased cAMP levels mediate the toxicity of both XMRV and the MCF 98D polytropic retrovirus in SY5Y cells.

Killing of mink cells by MCF 98D virus is dependent on the MCF virus *env* gene. To test the hypothesis that MCF virus toxicity was mediated by the interaction of Env with Xpr1, we generated hybrid viruses comprised of a noncytotoxic amphotropic retrovirus into which several cDNA clones of the *env* coding region of the MCF 98D virus were inserted. We produced virus from plasmids containing these clones by the transfection of the plasmids into MDTF cells and by growing the cells for >2 weeks to allow the virus to spread.

Mink cells were exposed to (i) medium harvested from MDTF cells, (ii) medium from MDTF cells producing an intact MCF virus or (iii) the amphotropic/MCF hybrid viruses, (iv) medium from NIH 3T3 cells producing amphotropic virus following transfection with plasmid pAMS, or (v) fresh culture medium only. The cells in each dish were trypsinized and replated at a 1:10 dilution every time they reached confluence. By day 3 after exposure, toxicity was evident in mink cells exposed to two of the amphotropic/MCF hybrid viruses and the intact MCF virus (two experiments). In contrast, during a month of observation, no difference in the growth rate or the appearance of cells exposed to medium from untransfected MDTF cells, fresh culture medium, medium containing the amphotropic virus, or medium from one of the three amphotropic/MCF virus clones tested was observed. We assume that the lack of cytotoxicity observed for one of the amphotropic/MCF virus clones was due to a disabling mutation, but we have not confirmed this. The same pattern of toxicity for the three amphotropic/MCF virus clones was observed after the infection of SY5Y cells, with toxicity due to two of the clones becoming apparent on day 8 after virus exposure. These results show that the cytotoxic effects of the MCF virus are linked to the MCF virus *env* gene and are consistent with a role of Xpr1 in MCF virus cytotoxicity.

Xpr1 has little or no role in phosphate uptake or its regulation. Inorganic phosphate (P_i) is a limiting nutrient in the environment, and cells from most organisms express multipass membrane-spanning proteins that actively concentrate phosphate within cells. The hydrophilic amino-terminal region of Xpr1 shows similarity to proteins involved in the regulation of phosphate uptake, e.g., yeast PHO81, *Neurospora* PHO85 and NUC-2, and rice and *Arabidopsis* SPX proteins (16, 28, 38). To test for a role for Xpr1 in phosphate uptake, we measured the kinetics of radiolabeled P_i uptake by 208F rat fibroblasts and Chinese hamster ovary (CHO) cells transduced with retroviral vectors that express hXpr1 or the Xpr1 ortholog from *Mus dunni* wild mice (mdXpr1). A retroviral vector expressing Pit-2, the cellular receptor for amphotropic MLV and a known sodium-dependent phosphate symporter (12), was used as a positive control, and the empty vector LXSN was used as a negative control. The level of P_i uptake by cells expressing hXpr1 was no different from that of cells transduced with the empty vector, while the level of P_i uptake by cells expressing rat Pit2 (rPit-2) (25) was dramatically increased (Fig. 8A and B). There was a small but reproducible decrease in the level of phosphate uptake by 208F and CHO cells expressing mdXpr1. These experiments indicate that hXpr1 and mdXpr1 are not primary phosphate transporters, as is rPit-2, but suggest the possibility that mdXpr1 has some ability to downregulate P_i uptake.

To further investigate the possible regulatory activity of mdXpr1, we measured the effect of mdXpr1 expression on the response of CHO cells to various concentrations of external P_i. We

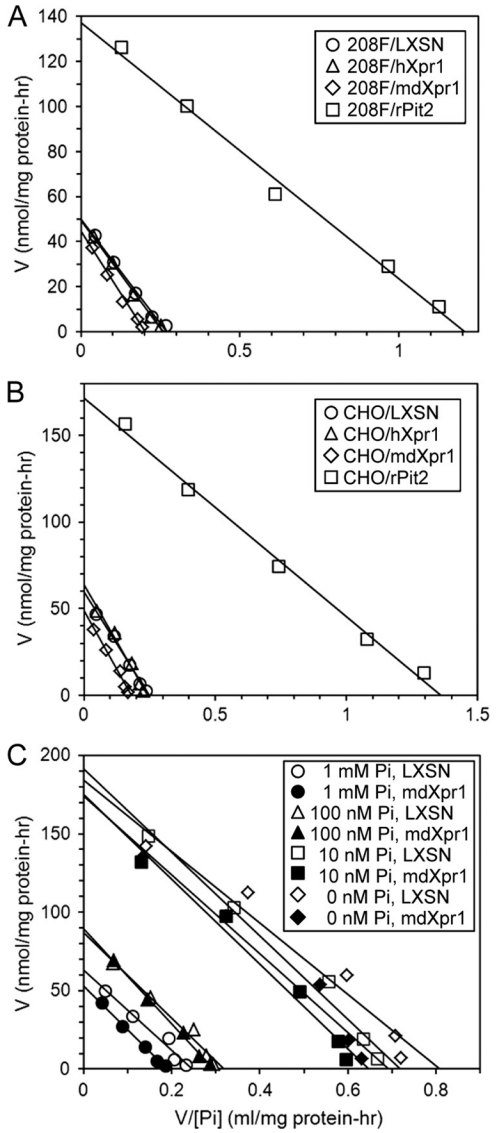

FIG 8 Expression of human or *Mus dunni* Xpr1 does not result in increased levels of phosphate uptake or significant alterations in the regulation of uptake. (A) Retroviral vectors encoding human Xpr1 (hXpr1) or *Mus dunni* Xpr1 (mdXpr1) were expressed in 208F rat cells that were used for phosphate uptake analysis. Eadie-Hofstee plots of phosphate uptake velocity (V) versus the velocity/phosphate concentration ratio ($V/[P_i]$) are shown. The y axis regression line intercept gives the V_{max} for phosphate uptake, and the slope is equal to $-K_m$. (B) The same phosphate uptake experiment described above for panel A was performed by using CHO cells. (C) 208F cells transduced with the mdXpr1-expressing vector or the empty vector LXSN were incubated with the indicated concentrations of phosphate overnight, and phosphate uptake was measured.

found that CHO cells exposed to culture medium without phosphate upregulated their endogenous phosphate uptake activity such that the V_{max} of phosphate uptake was increased by 2-fold after 4 h and by 5-fold after 15 h, showing that CHO cells actively regulate phosphate uptake. The responses of CHO cells to an overnight incubation with 0 or 10 nM P_i were similar whether they expressed mdXpr1 or not, and the responses to a 15-h exposure to 100 nM P_i were identical (Fig. 8C). There was still a small difference in the V_{max} between the populations of CHO cells cultured in 1 mM P_i (Fig. 8C), the concentration of P_i present in standard culture medium, consistent with our previous results (Fig. 8A and B).

To confirm that the Xpr1 orthologs were being expressed in CHO cells and that the lack of an alteration in the phosphate transport activity that we observed was not simply because the Xpr1 orthologs were not being expressed, we tested for Xpr1 function as a retrovirus receptor in CHO cells (Table 1). CHO cells are naturally resistant to xenotropic, polytropic, and amphotropic retrovirus infections, as confirmed with cells transduced with the empty vector (Table 1). The transfer of hXpr1 or mdXpr1 genes into the cells rendered them susceptible to xenotropic and polytropic, but not amphotropic, retroviruses, as expected. Human cells are somewhat less infectible by polytropic retroviruses, and this is reflected in the infectivity data for the human Xpr1 receptor. CHO cells transduced with the mXpr1 gene were susceptible to polytropic but not to xenotropic or amphotropic retrovirus infection, again as expected. These results show that hXpr1, mXpr1, and mdXpr1 are expressed in CHO cells transduced with the respective Xpr1 genes. Overall, our results indicate a limited role, if any, of Xpr1 in phosphate uptake or its regulation.

DISCUSSION

Xpr1 has been well characterized as a cellular receptor for polytropic and xenotropic MLVs, but its physiological function, aside from that predicted by its homology to the yeast signaling protein Syg1, has not been characterized. Xpr1 is a highly conserved protein with orthologs in animals, plants, and unicellular organisms, indicating its importance in basic cellular functions. This is underscored by the finding that the deletion of Xpr1 in mice is embryonic lethal (Lexicon Pharmaceuticals, personal communication), indicating an important role for Xpr1 in mammals.

Here we demonstrate that hXpr1 regulates cAMP in a manner analogous to that of known GPCRs and that it interacts with the Gβ subunit of the large G-protein complex. While a physiologic ligand for Xpr1 is unknown, we can force signaling through the Xpr1 pathway by the overexpression of Xpr1. Like known Gα-stimulatory GPCRs, Xpr1 activation increases intracellular levels

TABLE 1 *Homo sapiens*, *Mus musculus*, and *Mus dunni* Xpr1 clones function as retrovirus receptors when expressed in CHO cells[a]

Xpr1 ortholog	Vector titer for LAPSN pseudotype		
	Xenotropic retrovirus (NZB virus)	Polytropic retrovirus (MCF 98D virus)	Amphotropic retrovirus (4070A)
hXpr1	4×10^6	3×10^4	<1
mXpr1	40	5×10^7	<1
mdXpr1	2×10^6	6×10^7	<1
None	30	<1	<1

[a] Human, *Mus musculus*, and *Mus dunni* Xpr1 cDNAs were cloned into the LXSN retroviral expression vector, retroviruses were made from the vector plasmids by the transfection of HEK 293 cells with each vector and Moloney MLV *gag-pol* and VSV-G *env* genes, and CHO cells were exposed to the viruses and grown in G418 medium to select for the *neo* gene carried by the LXSN vector. To test for the ability of xenotropic, polytropic, and amphotropic retroviruses to infect CHO cells carrying the different *xpr1* genes, the cells were exposed to virus harvested from MDTF cells transduced with the LAPSN vector and the indicated replication-competent xenotropic or polytropic retroviruses or to the LAPSN vector produced by PA317 retrovirus packaging cells that express the 4070A amphotropic retrovirus Env protein. Two days later, the CHO cells were stained for alkaline phosphatase (expressed by the LAPSN vector) to determine the vector titer. Results are means of data from two to four experiments.

of cAMP, which acts as a second messenger and induces the downstream gene expression of CREB-responsive genes. However, unlike all other previously described GPCRs, Xpr1 contains eight putative transmembrane domains, as opposed to the canonical seven, and Xpr1 shows no sequence similarity to known GPCRs. Despite some similarity of Xpr1 to known phosphate transporters and phosphate transport regulators in yeast, *Neurospora*, rice, and *Arabidopsis*, we were unable to demonstrate a role for Xpr1 in phosphate uptake.

Interestingly, the expression of the 200-, 229-, and 248-aa C-terminal truncations of Xpr1, which lack most or all of the Xpr1 transmembrane domains, induced constitutive signaling. We hypothesize that this is due to the strong binding of Gβ by these truncated Xpr1 proteins, with the release of Gα into the cytoplasm, the constitutive activation of adenylate cyclase, and a resulting increase in cAMP levels. These results parallel previously reported findings with 400- and 417-aa C-terminally truncated Syg1 proteins in yeast (34) and indicate that the N termini of Xpr1 and Syg1 have similar functions despite having markedly different lengths and only 29% amino acid similarity (if multiple gaps in the alignment are ignored) or 17% similarity (if gaps are included).

We found that several retroviruses that utilize Xpr1 as a receptor for cell entry could inhibit Xpr1-mediated cAMP production, resulting in the apoptosis and death of some cell types. Interestingly, XMRV showed the most rapid toxic effect on SY5Y cells, while the MCF 98D virus showed the most rapid toxic effect on Mv1Lu mink lung cells. NZB virus had an intermediate effect on mink cells and had a lower level of toxicity, if any, than XMRV in SY5Y cells. All of these viruses can use the Xpr1 orthologs expressed in SY5Y and mink cells for cell entry. Presumably, the differential toxicity of these viruses is due largely to differences in their interactions with Xpr1 orthologs from different species. However, beyond initial receptor binding by Env, we do not know the mechanism of toxicity, which may involve the downregulation of Xpr1 signaling or the degradation of Xpr1-Env complexes during protein synthesis or following internalization from the cell surface.

While it seems clear now that XMRV is not associated with CFS, our study provides unique insights into a potential role for Xpr1 in neural biology. A role for deregulated cAMP signaling has clear precedents in other disease models and developmental observations. For example, mouse embryos lacking CREB, a major downstream transducer of G-protein signaling, exhibit excess apoptosis and degeneration of sensory and sympathetic neurons, and a CREB knockout is ultimately embryonic lethal (21). Our studies show that CREB is activated by Xpr1 signaling because CREB is the transcription factor that drives SEAP expression in the assay that we employed to measure cAMP levels. In addition, cAMP-modulating drugs have been shown to reverse neurodegeneration in cultured hippocampal neurons treated with amyloid β-peptide, a model of Alzheimer's disease (37). Moreover, mice infected with multiple neuropathic polytropic MLVs displayed increased expression levels of proinflammatory cytokines and chemokines, and neurodegenerative diseases such as Alzheimer's disease and multiple sclerosis induce similar cytokine and chemokine expressions (29).

Eurexpress Transcriptome Atlas data indicate that brain tissues show the highest Xpr1 expression levels in the mouse (6), lending support to the hypothesis that Xpr1 is involved in normal brain function. Notably, neuropathology can be induced in mice following infection with various retroviruses, and some studies have shown that polytropic retroviruses are neuropathic, while related ecotropic retroviruses that do not use Xpr1 as a receptor are not (29). However, neuropathology can also be found in mice following infection by some ecotropic retroviruses, such as CasBr-E MLV, that do not use Xpr1 as a receptor (32). The infection of mice with ecotropic retroviruses frequently results in recombination events leading to the production of polytropic retroviruses (32), and it would be interesting to determine if these recombinant viruses play a role in neurologic diseases induced by ecotropic retroviruses.

Our findings demonstrate the critical role which Xpr1 plays in mediating both xenotropic and polytropic retrovirus pathologies and further elucidate the function of Xpr1 in normal cells. However, there remain many questions regarding the normal physiological role of Xpr1 in animals, including what extracellular ligands might modulate Xpr1 activity. While our data indicate that Xpr1 provides a prosurvival signal to the cell, a more specific role for Xpr1 in signal transduction remains to be determined. It will be important to understand whether Xpr1 acts in a fashion analogous to that of other GPCRs and transmits a signal for a particular cellular process or whether it regulates GPCR and cAMP signaling in a more global fashion.

ACKNOWLEDGMENTS

This work was supported by the Fred Hutchinson Cancer Research Center (A.E.V. and A.D.M.), by pilot project funding from Core Center of Excellence in Hematology grant DK56465 (A.D.M.), by training grant T32 CA080416 from the National Cancer Institute (R.M.), and by funding from a summer undergraduate internship program (R.A.). J.-L.B. is currently supported by INSERM, the Association Française contre les Myopathies, and the Philippe Foundation.

We thank Linda Buck for providing the Cre-SEAP reporter vector, Bruce Chesebro for MCF 98D retrovirus and plasmid clones, and shared resources at the Fred Hutchinson Cancer Research Center for assistance with flow cytometry and DNA sequencing.

REFERENCES

1. **Aloia AL, et al.** 2010. XMRV: a new virus in prostate cancer? Cancer Res. **70**:10028–10033.
2. **Battini JL, Rasko JE, Miller AD.** 1999. A human cell-surface receptor for xenotropic and polytropic murine leukemia viruses: possible role in G protein-coupled signal transduction. Proc. Natl. Acad. Sci. U. S. A. **96**: 1385–1390.
3. **Biedler JL, Roffler-Tarlov S, Schachner M, Freedman LS.** 1978. Multiple neurotransmitter synthesis by human neuroblastoma cell lines and clones. Cancer Res. **38**:3751–3757.
4. **Bigner DD, et al.** 1981. Heterogeneity of genotypic and phenotypic characteristics of fifteen permanent cell lines derived from human gliomas. J. Neuropathol. Exp. Neurol. **40**:201–229.

4a. **Bradford MM.** 1976. A rapid and sensitive method for the quantitation of microgram quantities of protein utilizing the principle of protein-dye binding. Anal. Biochem. **72**:248–254.

5. **Chesebro B, Wehrly K.** 1985. Different murine cell lines manifest unique patterns of interference to superinfection by murine leukemia viruses. Virology **141**:119–129.
6. **Diez-Roux G, et al.** 2011. A high-resolution anatomical atlas of the transcriptome in the mouse embryo. PLoS Biol. **9**:e1000582.
7. **Dong B, et al.** 2007. An infectious retrovirus susceptible to an IFN antiviral pathway from human prostate tumors. Proc. Natl. Acad. Sci. U. S. A. **104**:1655–1660.
8. **Dorsam RT, Gutkind JS.** 2007. G-protein-coupled receptors and cancer. Nat. Rev. Cancer **7**:79–94.
9. **Hartley JW, Wolford NK, Old LJ, Rowe WP.** 1977. A new class of murine leukemia virus associated with development of spontaneous lymphomas. Proc. Natl. Acad. Sci. U. S. A. **74**:789–792.

10. **Jacobsen PF, Jenkyn DJ, Papadimitriou JM.** 1985. Establishment of a human medulloblastoma cell line and its heterotransplantation into nude mice. J. Neuropathol. Exp. Neurol. **44**:472–485.
11. **Kao FT, Puck TT.** 1968. Genetics of somatic mammalian cells. VII. Induction and isolation of nutritional mutants in Chinese hamster cells. Proc. Natl. Acad. Sci. U. S. A. **60**:1275–1281.
12. **Kavanaugh MP, et al.** 1994. Cell-surface receptors for gibbon ape leukemia virus and amphotropic murine retrovirus are inducible sodium-dependent phosphate symporters. Proc. Natl. Acad. Sci. U. S. A. **91**: 7071–7075.
13. **Knouf EC, et al.** 2009. Multiple integrated copies and high-level production of the human retrovirus XMRV (xenotropic murine leukemia virus-related virus) from 22Rv1 prostate carcinoma cells. J. Virol. **83**:7353–7356.
14. **Knox K, et al.** 2011. No evidence of murine-like gammaretroviruses in CFS patients previously identified as XMRV-infected. Science **333**:94–97.
15. **Kurre P, et al.** 1999. Efficient transduction by an amphotropic retrovirus vector is dependent on high-level expression of the cell surface virus receptor. J. Virol. **73**:495–500.

15a. **Lander MR, Chattopadhyay SK.** 1984. A *Mus dunni* cell line that lacks sequences closely related to endogenous murine leukemia viruses and can be infected by ecotropic, amphotropic, xenotropic, and mink cell focus-forming viruses. J. Virol. **52**:695–698.

16. **Lenburg ME, O'Shea EK.** 1996. Signaling phosphate starvation. Trends Biochem. Sci. **21**:383–387.
17. **Li Y, Cardona SM, Traister RS, Lynch WP.** 2011. Retrovirus-induced spongiform neurodegeneration is mediated by unique central nervous system viral targeting and expression of Env alone. J. Virol. **85**:2060–2078.
18. **Liberles SD, Buck LB.** 2006. A second class of chemosensory receptors in the olfactory epithelium. Nature **442**:645–650.
19. **Lo SC, et al.** 2010. Detection of MLV-related virus gene sequences in blood of patients with chronic fatigue syndrome and healthy blood donors. Proc. Natl. Acad. Sci. U. S. A. **107**:15874–15879.
20. **Lombardi VC, et al.** 2009. Detection of an infectious retrovirus, XMRV, in blood cells of patients with chronic fatigue syndrome. Science **326**: 585–589.
21. **Lonze BE, Riccio A, Cohen S, Ginty DD.** 2002. Apoptosis, axonal growth defects, and degeneration of peripheral neurons in mice lacking CREB. Neuron **34**:371–385.
22. **Metzger MJ, Holguin CJ, Mendoza R, Miller AD.** 2010. The prostate cancer-associated human retrovirus XMRV lacks direct transforming activity but can induce low rates of transformation in cultured cells. J. Virol. **84**:1874–1880.
23. **Miller AD, Buttimore C.** 1986. Redesign of retrovirus packaging cell lines to avoid recombination leading to helper virus production. Mol. Cell. Biol. **6**:2895–2902.
24. **Miller AD, Rosman GJ.** 1989. Improved retroviral vectors for gene transfer and expression. Biotechniques **7**:980–990.
25. **Miller DG, Edwards RH, Miller AD.** 1994. Cloning of the cellular receptor for amphotropic murine retroviruses reveals homology to that for gibbon ape leukemia virus. Proc. Natl. Acad. Sci. U. S. A. **91**:78–82.
26. **O'Neill RR, Buckler CE, Theodore TS, Martin MA, Repaske R.** 1985. Envelope and long terminal repeat sequences of a cloned infectious NZB xenotropic murine leukemia virus. J. Virol. **53**:100–106.
27. **Paprotka T, et al.** 2011. Recombinant origin of the retrovirus XMRV. Science **333**:97–101.
28. **Peleg Y, Aramayo R, Kang S, Hall JG, Metzenberg RL.** 1996. NUC-2, a component of the phosphate-regulated signal transduction pathway in *Neurospora crassa*, is an ankyrin repeat protein. Mol. Gen. Genet. **252**: 709–716.
29. **Peterson KE, Evans LH, Wehrly K, Chesebro B.** 2006. Increased proinflammatory cytokine and chemokine responses and microglial infection following inoculation with neural stem cells infected with polytropic murine retroviruses. Virology **354**:143–153.
30. **Peterson KE, et al.** 2008. Neurovirulence of polytropic murine retrovirus is influenced by two separate regions on opposite sides of the envelope protein receptor binding domain. J. Virol. **82**:8906–8910.
31. **Portis JL, Czub S, Robertson S, McAtee F, Chesebro B.** 1995. Characterization of a neurologic disease induced by a polytropic murine retrovirus: evidence for differential targeting of ecotropic and polytropic viruses in the brain. J. Virol. **69**:8070–8075.

31a. **Quade K.** 1979. Transformation of mammalian cells by avian myelocytomatosis virus and avian erythroblastosis virus. Virology **98**:461–465.

32. **Rosenberg N, Jolicoeur P.** 1997. Retroviral pathogenesis, p 475–585. *In* Coffin JM, Hughes SH, Varmus HE (ed), Retroviruses. Cold Spring Harbor Laboratory Press, Cold Spring Harbor, NY.
33. **Shaw G, Morse S, Ararat M, Graham FL.** 2002. Preferential transformation of human neuronal cells by human adenoviruses and the origin of HEK 293 cells. FASEB J. **16**:869–871.
34. **Spain BH, Koo D, Ramakrishnan M, Dzudzor B, Colicelli J.** 1995. Truncated forms of a novel yeast protein suppress the lethality of a G protein α subunit deficiency by interacting with the β subunit. J. Biol. Chem. **270**:25435–25444.
35. **Tailor CS, Nouri A, Lee CG, Kozak C, Kabat D.** 1999. Cloning and characterization of a cell surface receptor for xenotropic and polytropic murine leukemia viruses. Proc. Natl. Acad. Sci. U. S. A. **96**:927–932.
36. **Urisman A, et al.** 2006. Identification of a novel gammaretrovirus in prostate tumors of patients homozygous for R462Q RNASEL variant. PLoS Pathog. **2**:e25.
37. **Vitolo OV, et al.** 2002. Amyloid β-peptide inhibition of the PKA/CREB pathway and long-term potentiation: reversibility by drugs that enhance cAMP signaling. Proc. Natl. Acad. Sci. U. S. A. **99**:13217–13221.
38. **Wang C, et al.** 2009. Involvement of OsSPX1 in phosphate homeostasis in rice. Plant J. **57**:895–904.
39. **Yang YL, et al.** 1999. Receptors for polytropic and xenotropic mouse leukaemia viruses encoded by a single gene at Rmc1. Nat. Genet. **21**: 216–219.
40. **Yoshimura FK, Wang T, Nanua S.** 2001. Mink cell focus-forming murine leukemia virus killing of mink cells involves apoptosis and superinfection. J. Virol. **75**:6007–6015.
41. **Zhao X, Yoshimura FK.** 2008. Expression of murine leukemia virus envelope protein is sufficient for the induction of apoptosis. J. Virol. **82**: 2586–2589.